

1   **Root hairs shape microbiome structure and network interactions upon drought stress**

3   Zhenghong Wang<sup>1#</sup>, Zewen Li<sup>1#</sup>, Jingxuan Zhai, Xianli Tang<sup>1</sup>, Kaixiang Guan, and Yi Song<sup>1\*</sup>

5   **Authors:**

6   <sup>1</sup>Institute of Plant and Food Science, Department of Biology, Southern University of Science and  
7   Technology (SUSTech), Shenzhen, Guangdong 518055, China

8   \*Correspondence: Yi Song (songy3@sustech.edu.cn).

9   <sup>#</sup>Contributed equally.

11   **Abstract**

12   Drought is one of the most serious abiotic stresses which also shifts the composition of root  
13   associated microbiomes. However, there is a lack of genetic evidence regarding whether and how  
14   plant genetic effects positively reshape drought induced microbiome changes. Root hairs play  
15   essential roles in water uptaking, but whether root hairs also orchestrate microbiome re-shaping  
16   process during drought stress is unknown. By utilizing genetic mutants with enhanced or decreased  
17   root hair densities, we detected a significant effect of plant genetic effect on drought induced  
18   microbiome changes. In addition, the hairy mutant (*gl2*) triggers a deterministic dominant process  
19   during drought induced microbiome re-assembly, which further confirms the involvement of host  
20   effects in re-shaping drought induced microbiome changes. *Rhizobiaceae* strains were detected as  
21   key biomarker species positively correlated with root hair densities. Moreover, the *gl2* mutant also  
22   shapes more complex microbiome co-occurrence networks, with more *Rhizobiaceae* hubs. Our  
23   findings unveil the novel roles of root hairs in shaping microbiome structure and network  
24   interactions upon drought stress, particularly through regulating the abundance and network  
25   centrality of *Rhizobiaceae* strains. Root hair related mutants also broadly affect root metabolome  
26   upon drought stress. Understanding the physiological and microbial ecological basis of host  
27   mediated microbiome re-shaping under drought helps develop microbiome engineering approaches  
28   to combat climate changes.

29   

30   **Introduction**

31   Plant roots are surrounded by highly diverse soil microbial communities, and their co-evolution  
32   is crucial for the function of rhizosphere ecosystem and plant fitness<sup>1-4</sup>. Different plant ecotypes or  
33   cultivars share common and sometimes heritable, microbiome features<sup>5-7</sup>, indicating that hosts can  
34   selectively shape a "core microbiome". Additionally, plants can even actively reshape the  
35   microbiome in response to various stresses to enhance fitness<sup>8</sup>. However, our understanding about  
36   the regulations between genes and microbiome ecosystems, and their consequences for plant fitness,  
37   are still in its infancy. Drought stress causes significant threat to global agricultural production, with  
38   estimates indicating that over 50% of arable land will be affected by drought by 2050<sup>9</sup>. Drought also  
39   profoundly disrupts soil microbiomes and plant-associated microbiomes across various plant

40 species and ecosystems<sup>10,11</sup>, and prolonged drought stress even dampens rhizosphere ecosystem  
41 resilience after drought recovery<sup>12</sup>. Currently, it remains largely elusive how host reshapes root  
42 associated microbiomes under drought stress.

43

44 Numerous studies indicate host effects are positively involved in reshaping drought induced root  
45 microbiome changes, although we still lack solid genetic evidence to support this. Drought stress  
46 exerts a much stronger influence on the composition of root-associated microbiomes than that on  
47 bulk soil microbiomes<sup>10</sup>. Furthermore, the effect of drought on root-associated microbiomes varies  
48 in different plant development stages (flowering or not)<sup>13</sup>, indicating the impact of plant  
49 developmental stages on drought-induced microbiome reshaping. Integrated multi-omics  
50 approaches have suggested that glycerol 3-phosphate (G3P) and iron are potential metabolic cues  
51 affecting drought induced microbiomes shifts<sup>13,14</sup>. Studies in different wild species and crops have  
52 demonstrated that drought stress can enrich certain microbes, such as actinobacteria (especially  
53 *Streptomyces*), which may enhance host drought tolerance<sup>12,15,16</sup>. Recent research has also shown  
54 that tree seedlings infected with different microbiomes from dry or warmer environments exhibit  
55 enhanced fitness over multiple years<sup>4</sup>. These studies suggest that microbiome engineering or  
56 "microbiome breeding" approaches hold promise as environmentally friendly way to help plants  
57 adapt to climate changes<sup>17</sup>. Further genetic studies could provide deeper mechanistic understanding  
58 of how host positively regulates drought-triggered microbiome changes, which is crucial for  
59 harnessing microbiome to combat drought stress<sup>18</sup>.

60

61 Plant genetic studies have provided valuable insights into how plants regulate microbiome  
62 composition. For example, our previous genetic screening identified a receptor-like kinase,  
63 FERONIA, which can regulate the colonization of beneficial Pseudomonads<sup>19</sup>, which might be  
64 related to pathogen triggered recruitment of beneficial Pseudomonads. A pioneering genetic study  
65 demonstrated that *Arabidopsis* mutants disrupting several hormone signaling pathways could alter  
66 microbiome structure<sup>20</sup>. This provided the first solid genetic evidence that plants can shape root-  
67 associated microbiome. Moreover, by using quadruple mutant to dampens multiple plant immune  
68 pathways, a previous study revealed the critical roles of innate immunity in maintaining microbiome  
69 homeostasis and plant health<sup>21,22</sup>. Leveraging the power of genetic manipulations in *Arabidopsis*,  
70 researchers have further revealed that various plant signaling pathways influence microbiome  
71 structure, including epigenetic modifications<sup>23,24</sup>, small RNA generating<sup>25</sup> and diverse metabolic  
72 pathways<sup>26,27</sup>. Although plant genetic tools have been extensively employed to dissect the regulation  
73 mechanisms of microbiome composition and changes, genetic studies regarding how plants  
74 positively reshape microbiomes under drought stress are still lacking.

75

76 Root hairs are essential for water and nutrient uptake, and also serve as the frontline cells of host-  
77 microbiome interactions<sup>28,29</sup>. Additionally, plants secrete approximately 20-30% of their

78 photosynthetic carbon source as root exudates into the rhizosphere, with root hairs playing a vital  
79 role in this process<sup>30</sup>. We thus hypothesized that root hairs might orchestrate microbiome sculpting  
80 upon drought stress during long-term evolution. The well characterized genetic regulation pathways  
81 of root hair development enable us to obtain mutants with altered root hair densities to study their  
82 effects on drought induced microbiome changes. The master transcription factor GLABRA 2  
83 maintains a non-hair cell fate and negatively regulates root hair initiation and development<sup>31</sup>. In  
84 contrast, a group of basic helix-loop-helix transcription factors, *ROOT HAIR DEFECTIVE 6 (RHD6)*  
85 and its homolog gene *RHD6-LIKE 1 (RSL1)*, positively regulate the expression of *RSL2-5* genes to  
86 promote root hair development<sup>32</sup>. We thus utilized genetic mutants with different root hair densities  
87 to dissect the role of root hairs in regulating drought induced microbiome changes. The objectives  
88 of this study are: 1) to decipher the effect of genetic mutations related to root hairs on microbiome  
89 composition under drought stress; 2) to identify keystone taxa or microbes influenced by root hairs  
90 under drought stress; 3) to profile potential metabolic cues related to root hair-mediated community  
91 assembly; 4) to validate the effects of root hair-regulated microbes on plant growth and drought  
92 tolerance. This study will enhance our understanding of the genetic and physiological mechanisms  
93 involved in plant mediated reshaping of microbiome under drought.

94

## 95 **Results**

### 96 **Mutants with different root hair densities shift microbiome composition under drought stress**

97 To provide genetic evidence about the role of root hairs in shaping drought induced microbiome  
98 changes, we employed the *rsl2 rsl4*<sup>33</sup> double mutant (complete loss of root hairs), the *g12*<sup>34</sup> mutant  
99 (significantly increased root hair density), and wild type *Arabidopsis* for our microbiome profiling  
100 analysis (Fig. 1a). In order to mimic a highly diverse natural soil microbiome and enrich drought  
101 adapted soil microbes, we mixed natural soils from a tropical rainforest soil (expected to have high  
102 microbial diversity) and a dry hot valley in southwest China (expected to have drought-adapted  
103 microbes) as our experimental natural soil. To more thoroughly reflect microbiomes changes in  
104 different compartments, we sampled both root (thoroughly washed roots) and rhizosphere (closely  
105 attached soil on root surface) microbiome samples for each group in our study.

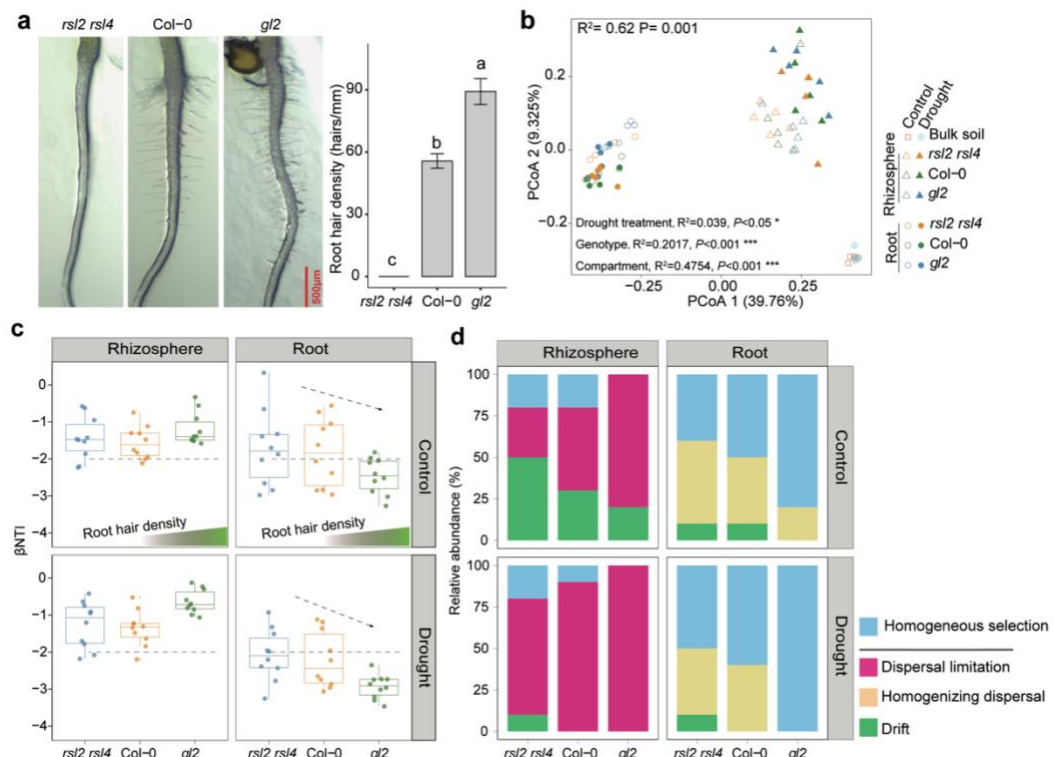
106

107 A total of 15,332,970 reads were obtained from 70 samples, including rhizosphere, root, and bulk  
108 soil (soil under same treatment procedure without plants) samples (Supplementary Table 1). After  
109 filtering, denoising, chimaera removal, and taxonomic annotation (based on the SILVA database  
110 using a pre-trained naive Bayes classifier) using DADA2<sup>35</sup>, we obtained 5174 amplicon sequence  
111 variants (ASVs) from all samples (Supplementary Table 2). We observed significant differences in  
112 microbiome composition between root-associated microbiomes and bulk soil (BS) samples at both  
113 phylum and family levels, indicating a clear rhizosphere effect on microbiome composition  
114 (Supplementary Fig. 1a, b). We found that *g12* show enhanced alpha diversity of root microbiomes

115 of samples from the control (Supplementary Fig. 1c), suggesting a positive role of root hairs in  
 116 maintaining microbial diversity.

117

118 Principal coordinated analysis (PCoA) based on Bray–Curtis dissimilarities were performed for  
 119 all samples. Our results showed that samples belonging to different compartments (like bulk soil,  
 120 root, and rhizosphere) clustered in distinct groups (Fig. 1b;  $R^2=0.4757$ ,  $P <0.001$ ), as well as a  
 121 significant separation among treatments (Fig. 1b;  $R^2 = 0.039*$ ,  $P <0.05$ ). Both drought stress and  
 122 root compartments (root and rhizosphere) had substantial effects on microbiome composition,  
 123 consistent with previous reports<sup>36,37</sup>. Interestingly, we found that plant genotypes also exert  
 124 significant influence on microbiome compositions (Fig. 1b;  $R^2 = 0.207***$ ,  $P <0.001$ ). These results  
 125 suggest that both root hair related mutants (genotypes) and drought stress (treatments) jointly shape  
 126 root-associated microbiome changes upon drought stress.



127

128 **Fig. 1 Root hair mutants shift microbiome composition under drought stress.** a Photos and quantification of  
 129 root hair densities of the 5-day-old roots of Col-0, rsl2 rsl4 and gl2. Data are represented as mean (bar)  $\pm$  standard  
 130 error of mean (error bar). Experiment was repeated twice with consistent results. Different letters represent the  
 131 significant ( $p < 0.05$  corrected using Bonferroni method, one-way ANOVA followed by LSD test) differences among  
 132 genotypes (N=40 biological replicates). b. Principal coordinates analysis based on Bray–Curtis dissimilarity that  
 133 calculated from the relative abundance matrices at ASV level (PERMANOVA by adonis, n=5 replicates for each  
 134 individual group). c The  $\beta$ -nearest taxon indexes ( $\beta$ -NTI) in different genotypes. Each dot represents the  $\beta$ -nearest  
 135 taxon index calculated from each pairwise sample in each genotype and treatment condition. The dotted line  
 136 represents the cutoff for determining deterministic ( $|\beta$ -NTI|>2) and stochastic ( $|\beta$ -NTI|<2) processes. Box plots show  
 137 the median (horizontal bar), 25th (bottoms of boxes) and 75th (tops of boxes) quartiles range (QR), and non-outlier

138 data value (upper and lower whiskers) of  $\beta$ -nearest taxon index value in each group. d Percentage of relative  
139 influence of each community assembly cues were defined as proportion of pairwise samples governed by each  
140 process. The horizontal line in the legend represents the boundary between the main ecological processes driven by  
141 deterministic processes (above) and stochastic processes (below).

142 ***gl2* mutant drives a deterministic microbiome assembly process during drought stress**

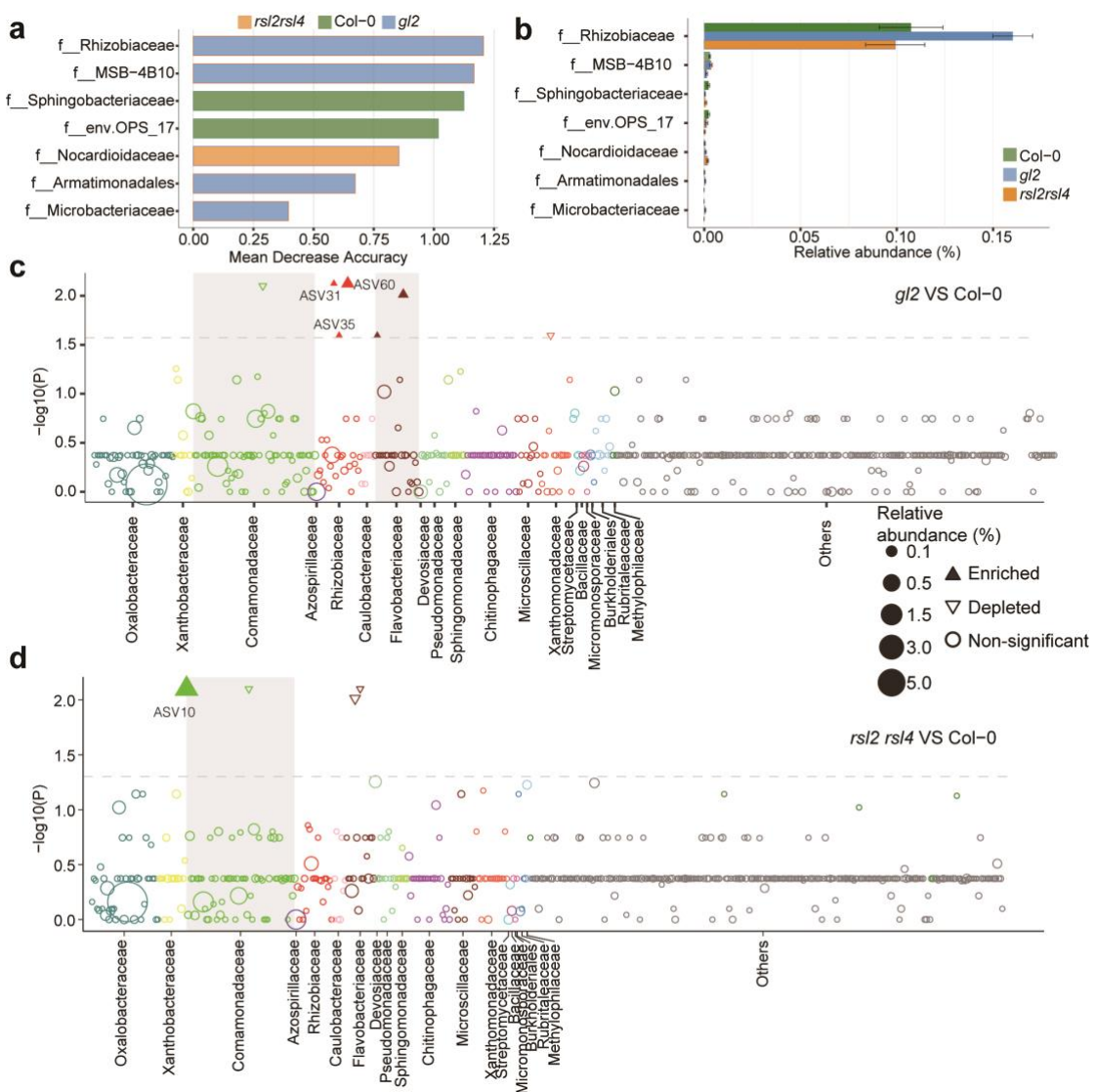
143 Understanding the assembly cues of microbial communities helps us understand the factors that  
144 influence community changes<sup>38</sup>. To assess whether plant root hair related genetic effects contribute  
145 to a deterministic process in microbiome assembly, we calculated the  $\beta$ -nearest taxon index ( $\beta$ NTI)  
146 indexes in the microbiome samples of root hair related mutants ( $|\beta$ NTI| > 2 indicates a deterministic  
147 process<sup>38</sup>). For rhizosphere samples, a stochastic process (-2 <  $\beta$ NTI < 0) governed the assembly of  
148 genotype-specific bacterial communities in both the control and drought-treated groups (Fig. 1c),  
149 suggesting a relatively weak rhizosphere effect in regulating rhizosphere microbiome changes. In  
150 contrast, we detected a stronger effect of genotype on root microbiome assembly. With the increase  
151 in root hair density, the root microbiome assembly shifted from a co-governed pattern by stochastic  
152 and deterministic processes (in roots of *rsl2 rsl4* and Col-0) to a pattern primarily governed by  
153 deterministic process (in roots of *gl2*). Importantly, the assembly of bacterial communities in the  
154 roots of *gl2* was completely governed by a deterministic process ( $\beta$ NTI < -2) under drought  
155 conditions (Fig. 1c). That means enhanced root hair density has strong deterministic influence on  
156 drought induced root microbiome changes.

157 We further calculated the Bray-Curtis-based Raup-Crick index (RCbray) to quantify the  
158 contribution of different community assembly cues. This index allowed us to assess the proportion  
159 of pairwise community comparisons dominated by each process. In rhizosphere samples, dispersal  
160 limitation ( $\beta$ NTI < -2 and RCbray > 0.95) governed the stochastic process in all genotypes under  
161 drought (Fig. 1d). Interestingly, for root samples, the deterministic process were dominated by  
162 homogenous selection (Fig. 1d;  $\beta$ NTI < -2). Importantly, the relative influence of homogenous  
163 selection in the assembly of bacterial communities was much higher (75% - 100%) in *gl2* than in  
164 *rsl2 rsl4* (below 50%) and Col-0 (approximately 50%). Our results provided genetic evidence about  
165 the involvement of plant effects in deterministic microbiome assembly under drought stress.

166 ***Rhizobiaceae* are the key taxa regulated by root hairs under drought stress**

167 To further explore the key taxa influenced by root hairs under drought conditions, we analyzed  
168 the relative abundance of different taxonomic levels among genotypes. Mutants exhibited clear  
169 shifts at the family level (Supplementary Fig. 1d). We found that the abundance of *Rhizobiaceae*  
170 was significantly higher in *gl2* than *rsl2 rsl4* under drought stress (Supplementary Fig. 2b). Notably,  
171 by using a RandomForest predicting<sup>39</sup>, we identified *Rhizobiaceae* as the most effective family in  
172 distinguishing the three genotypes (Fig. 2a), and also with the highest abundance among all  
173 biomarker families identified (Fig. 2b).

174 We further performed differential abundant analysis of ASVs between individual mutants and  
 175 Col-0. We found that the differential ASVs (DA-ASVs) from rhizosphere samples between the two  
 176 root hair mutants and Col-0 were distributed across multiple families, regardless of whether it was  
 177 in the drought or control group (Supplementary Fig. 2a-d). However, for DA-ASVs in root samples  
 178 were enriched in a few families, especially under drought condition (Supplementary Fig. 2e, f; Fig.  
 179 2c, d). We detected 5 significantly enriched ASVs in *gl2*, and 3 of them belong to *Rhizobiaceae* (Fig.  
 180 2c). Only 1 ASV (belonging to *Comamonadaceae*) was enriched in the root microbiome of *rsl2 rsl4*  
 181 (Fig. 2d). Collectively, our machine learning (RandomForest) based biomarker prediction, as well  
 182 as differential abundance analysis at the family level, all support that *Rhizobiaceae* are major  
 183 biomarker taxa regulated by root hairs under drought stress.



184

185 **Fig. 2 Biomarker taxa and species between mutants and Col-0.** a-b A total of 7 marker families were identified  
 186 under drought conditions by Kruskal-Wallis rank sum test and random forest classification (a) and their  
 187 corresponding relative abundances (b) in each genotype. In bar plot, data are represented as mean (bar)  $\pm$  standard  
 188 error of mean (error bar). c-d Manhattan plot showing the differential abundance ASVs enriched or depleted in the

189 roots of *gl2* (c) and *rsl2 rsl4* (d) compared to Col-0 (Wilcoxon rank sum test, unadjusted  $p < 0.05$ ) under drought  
190 condition. n=5 biological replicates for microbiome analysis in each genotype and treatment conditions. Each dot  
191 and triangle represent each ASV. ASVs were colored according to the taxonomic family. Size of each dot or triangle  
192 represent the relative abundance of each ASV. Solid upward triangles indicate the ASVs enriched in the roots of  
193 mutant. Hollow downward triangles represent the ASVs depleted in the mutants.

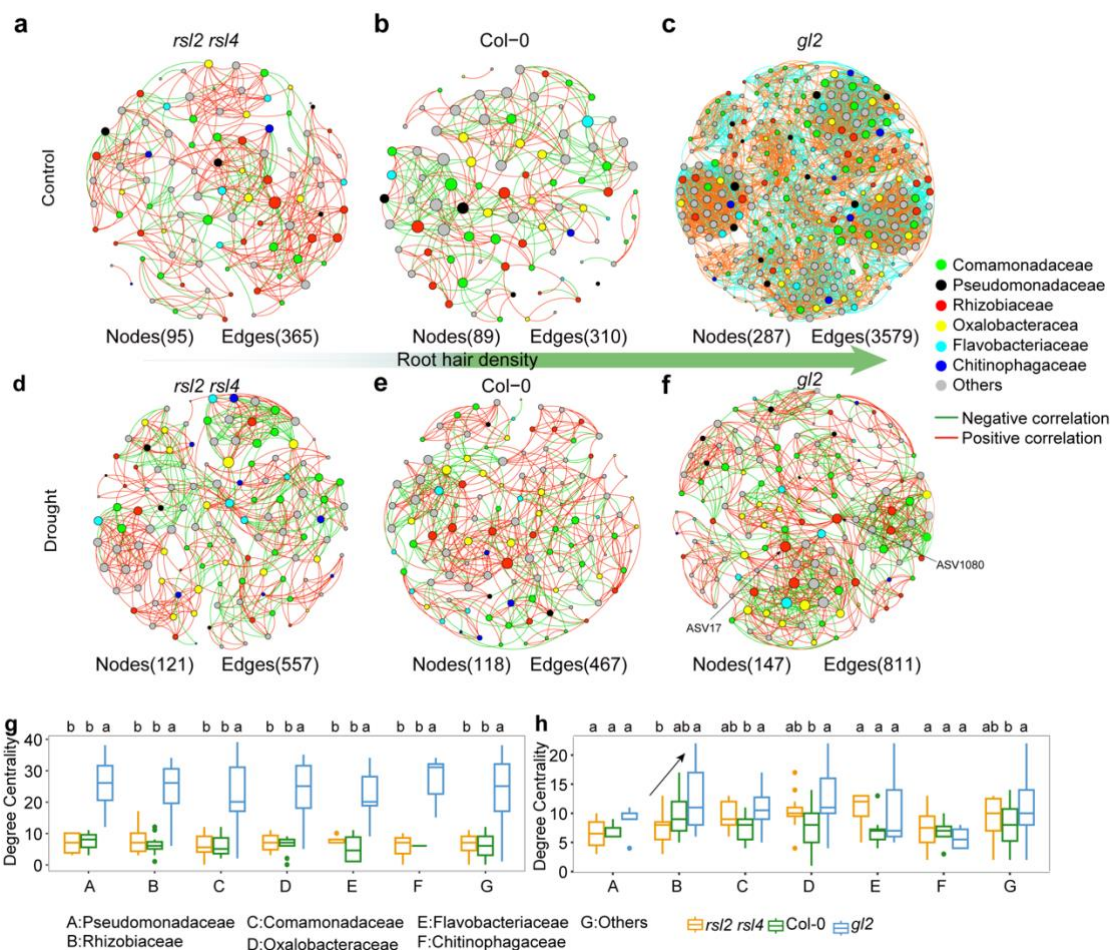
194 ***gl2* mutant affects the network importance of *Rhizobiaceae* nodes**

195 Complex microbe-microbe interactions substantially affect network structure and stability, which  
196 further affect community function<sup>40</sup>. Network analysis is widely used to identify keystone taxa that  
197 play important roles in shaping microbial community structure and affecting community  
198 functions<sup>41,42</sup>. Considering that we only observed a deterministic assembly process in root but not  
199 rhizosphere microbiome (Fig. 1c, d), we subsequently focused on the network interactions within  
200 root microbiome. To further explore whether and how root hairs affect network interactions in root  
201 microbiomes, we constructed the co-occurrence networks based on Spearman's correlations (with a  
202 correlation coefficient threshold of 0.7,  $P_{FDR} < 0.05$ ) between paired ASVs in the root microbial  
203 communities within each genotype. We found that, compared to Col-0 (Fig. 3a, nodes under  
204 control=89; Fig. 3d, nodes under drought=118), the hairy mutant *gl2* has much larger (total number  
205 of nodes) and more complex microbiome networks under both control (Fig. 3c; nodes=287) and  
206 drought (Fig. 3f; nodes=147) conditions. Additionally, the network connectivity (total number of  
207 edges) and average connectivity (average links/degree per nodes) are also higher in the *gl2* mutant  
208 compared to Col-0 and *rsl2 rsl4* (Fig. 3a-f; Supplementary Table 3). By contrast, there was no  
209 significant difference in network size and connectivity between the co-occurrence networks of *rsl2*  
210 *rsl4* and Col-0 (Fig. 3a, b, d, e). Our data strongly supports that the increase in root hair density  
211 leads to increased complexity in the networks of root microbiomes, both under control and drought  
212 conditions.

213 Differences in the network topological properties of different nodes (ASVs) determine the  
214 importance of each node in the network. Degree centrality (the number of edges connected to the  
215 node) and closeness centrality (average length of the shortest path between the node and all other  
216 nodes) are broadly used to describe the importance of network nodes. We observed that ASVs  
217 belonging to the top six families (top 10 abundance-ranked and the top 10 network-node-count-  
218 ranked overlapping families from all genotypes) exhibited significantly higher mean degree  
219 centrality in the network of *gl2* under control, compared to Col-0 and *rsl2 rsl4* (Fig. 3g; ANOVA  
220 analysis followed by Fisher's LSD test,  $P < 0.05$  corrected using Bonferroni method). The ASVs  
221 belonging to *Rhizobiaceae*, *Comamonadaceae*, and *Oxalobacteraceae* showed significant  
222 differences in mean degree centrality in *gl2* compared to Col-0 under drought conditions. The mean  
223 degree centrality of the ASVs belonging to *Rhizobiaceae* consistently increased from *rsl2 rsl4*, Col-  
224 0 to *gl2*, indicating a crucial role of root hairs in maintaining the network importance of  
225 *Rhizobiaceae* nodes (Fig. 3h).

226 Hub nodes (ASVs) were usually identified based on their degree centrality, closeness centrality,

227 and betweenness centrality indexes<sup>43</sup>. We further analyzed all those indexes related centrality, and  
 228 two hub ASVs were identified in the network of *gl2* under drought treatment, and both are belonging  
 229 to *Rhizobiaceae* (Supplementary Fig. 3). We also detected increased interactions with *Rhizobiaceae*  
 230 nodes in *gl2* under drought conditions. In the co-occurrence network of *gl2*, the edges interacting  
 231 with the ASVs belonging to *Rhizobiaceae* increased from 16.2% to 24.7% from control to drought  
 232 condition (Supplementary Table 3). Collectively, our results suggest that increased root hair density  
 233 enhances network complexity and importance of ASVs belonging to *Rhizobiaceae* in the root  
 234 microbiome.



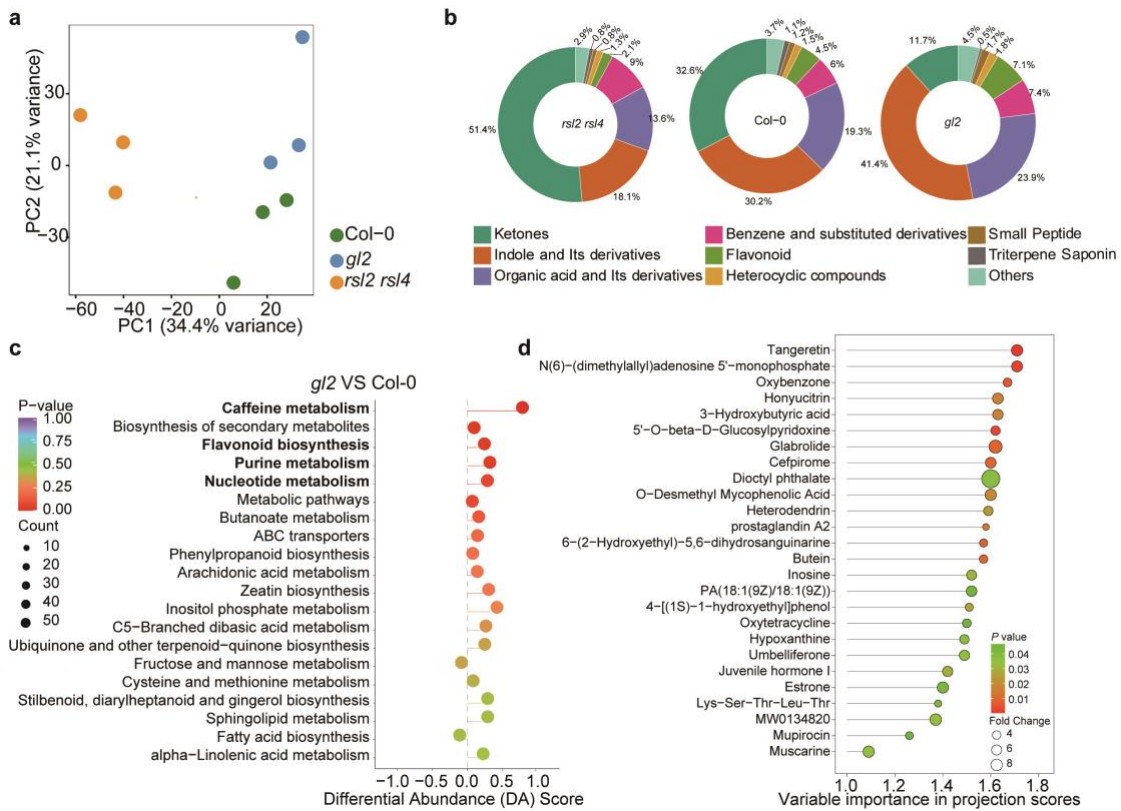
235  
 236 **Fig. 3 Changes in the microbial co-occurrence networks of root-associated samples of root hair mutants and**  
 237 ***Col-0*.** a-c Co-occurrence networks of microbiomes in the root samples of *rsl2 rsl4* (a), *Col-0* (b), *gl2* (c) root samples  
 238 under control. Red dots indicate nodes belonging to *Rhizobiaceae*. d-f Co-occurrence networks of microbiomes in the  
 239 rhizosphere samples of *rsl2 rsl4* (d), *Col-0* (e), *gl2* (f) under drought condition. The exact numbers of nodes and  
 240 edges were indicated below each graph. The arrow indicated the hub nodes within each network. g-h The  
 241 distributions of degree centrality of ASVs from the top 6 families across microbiome networks in the roots of  
 242 different genotypes under control (g) and drought conditions (h). The different letters represent the significant ( $p <$   
 243 0.05 corrected using Bonferroni method, one-way ANOVA followed by LSD test) differences among genotypes.  
 244 Box plots show the median (horizontal bar), 25th (bottoms of boxes) and 75th (tops of boxes) quartiles range (QR),  
 245 and non-outlier data value (upper and lower whiskers) of ASV's degree centrality within each family.

246 ***gl2* mutant broadly shifts the composition of root metabolome and enriches flavonoids**

247 Root exudates play a pivotal role in shaping genotype- or stress-specific microbiomes<sup>44,45</sup>. To  
248 investigate the potential metabolic cues related to *gl2**gl2* mediated microbiome re-shaping under  
249 drought stress, we conducted non-targeted metabolomics analysis of chemical compositions in the  
250 roots of *gl2*, *rsl2 rsl4*, and Col-0. A total of 3920 compounds were identified in root samples from  
251 different genotypes. Principal component analysis (PCA) revealed significant differences in the  
252 biochemical composition of root metabolites ( $R^2= 0.58$ ,  $P<0.05$ , PERMANOVA by adonis) among  
253 these genotypes (Fig. 4a). The content of flavonoids is significantly higher (7.1%) in the roots of  
254 *gl2* compared to that in Col-0 (4.5%) and *rsl2 rsl4* (2.1%) (Fig. 4b). Conversely, the relative content  
255 of ketones was higher in the roots of *rsl2 rsl4* mutant (51.4%) compared to Col-0 (32.6%), but lower  
256 in the roots of *gl2* mutant (11.7%) (Fig. 4b). Indole and its derivatives, as well as organic acid and  
257 its derivatives, were higher in the root of *gl2* compared to Col-0, but lower in *rsl2 rsl4*. The  
258 metabolome profiling results suggest that mutations in root hair development can significantly alter  
259 the composition of metabolites in roots under drought.

260

261 Subsequently, differentially abundant metabolites (DMs) were identified based on variable  
262 importance in projection scores ( $VIP > 1.0$ ) and fold changes ( $\log FC > 0$ ) of the relative abundances  
263 ( $P<0.05$ ). A total of 383 DMs were identified between *gl2* and Col-0 (Supplementary Table 4), and  
264 964 DMs were identified between *rsl2 rsl4* and Col-0 (Supplementary Table 5). Enrichment analysis  
265 was further performed based on DMs in *rsl2 rsl4* and *gl2*, respectively. Consistent with the increase  
266 in relative content of overall flavonoids, the DMs in the roots of *gl2* are enriched in pathways  
267 associated with flavonoid biosynthesis, as well as pathways related to caffeine metabolism, purine  
268 metabolism, and nucleotide metabolism (Fig. 4c). In contrast, the DMs in *rsl2 rsl4* are mainly  
269 enriched in pathways related to C5-Branched dibasic acid metabolism, plant hormone signal  
270 transduction, butanoate metabolism, and monobactam biosynthesis (Supplementary Fig. 4a). A  
271 previous study showed that flavonoids accumulation in roots can induce the chemotaxis of  
272 *Aeromonas* and enhance plant dehydration resistance<sup>46</sup>. Furthermore, flavonoids (e.g., naringenin)  
273 are well-known for their effects on inducing the expression of rhizobia nod genes in leguminous  
274 plants, as well as the chemoattraction of rhizobia towards the roots<sup>47</sup>. In the present study, tangeretin  
275 (a flavonoid molecule) in the roots of *gl2* exhibited the highest VIP value (Supplementary Table 3;  
276  $P < 0.001$ ) among the DMs with a more than 3 folds enrichment compared to Col-0 (Fig. 4d,  
277 Supplementary Fig. 4b). The above results comprehensively revealed the metabolome changes in  
278 *gl2* during drought stress, including the enrichment of flavonoid compounds which were reported  
279 to be related to rhizobia colonization in leguminous plants.



280

281 **Fig. 4 Metabolomic profiling of root samples from different genotypes under drought stress.** **a** Principal  
 282 component analysis (PCA) of metabolites detected in the roots of Col-0, gl2 and rsl2 rsl4 ( $p < 0.001$ , permutational  
 283 multivariate analysis of variance (PERMANOVA) by Adonis). N=3 biological replicates. **b** Relative content of  
 284 different metabolites classes in the roots of Col-0, gl2 and rsl2 rsl4. **c** Enriched pathways of differentially abundant  
 285 metabolites (DMs) in gl2 compared to Col-0 under drought condition. The differential abundance (DA) score  
 286 represents the number of changed DMs relative to the total numbers of metabolites within each pathway. Colors  
 287 indicate p-values and size of each dot indicate the number of metabolites. **d** Variable importance of projection (VIP)  
 288 scores of all the DMs (fold change  $> 2$  are displayed) in the roots of gl2. The colors indicate p-value. The size of  
 289 each circle represents the fold changes of relative contents in gl2 relative to Col-0.

290

## 291 Discussion

292 In the era of the host-microbiome holobiont, understanding how host genetics facilitate the  
 293 recruitment of beneficial microbes under stresses is a fundamental question critical for engineering  
 294 plant microbiome. To address this, we need to integrate genetic approaches, multiple-omics and  
 295 reductionist based confirmations. Thanks to the power and low cost of plant genetics approaches,  
 296 previous studies have been well established that plant genetic effects positively contributes to  
 297 recruiting disease suppressive microbes<sup>8,19,48</sup>. In contrast, while drought is the most serious abiotic  
 298 stress which drastically disturbs root associated microbiome, whether and how plant genetic effects  
 299 positively recruit stress-alleviating microbes during drought is largely unknown. By taking  
 300 advantage of elaborately selected genetic mutants with a gradient of root hair densities, we were  
 301 able to confirm the crucial role of plant root hairs in positively re-shaping drought triggered  
 302 microbiome changes. Our microbiome composition and network analyses revealed that *Rhizobiaceae*

303 are the major family regulated by root hairs. Our work supports the essential roles of plant genetic  
304 effects in positively re-shaping a drought alleviating microbiome, and furthers our understanding  
305 about the “cry for help” phenomenon during abiotic stress.

306

307 Similar to gut microvilli, plant root hairs substantially increase root surface area and play essential  
308 roles in nutrient and water uptake. Conventional crop breeding programs typically prioritize high  
309 root hair density and length as desirable traits in agriculture, primarily from a nutrient uptake  
310 perspective<sup>49,50</sup>. However, our work reveal a critical novel role of root hairs in orchestrating the  
311 beneficial interactions with root associated microbiomes. This is reminiscent of a recent study which  
312 surveyed the root cell type specific transcriptome responses to beneficial *Pseudomonas simiae*  
313 WCS417 in roots, and found that root hairs show special immune responsiveness to WCS417<sup>51</sup>.  
314 Root hair related mutants also dampen the immune responses and compatible interactions with  
315 WCS417, highlighting the crucial roles of root hairs in sensing and regulating the interactions with  
316 beneficial microbes<sup>51</sup>. Furthermore, our recent single-nucleus RNA-seq analysis discovered that  
317 beneficial microbes (*Pseudomonas simiae* WCS417) and pathogenic microbes (*Ralstonia*  
318 *solanacearum* GMI1000) trigger very distinct (only 11.84% overlap) transcriptome responses in  
319 root hairs (trichoblasts)<sup>52</sup>. Beneficial WCS417 promotes the expression of growth-related GO terms  
320 related to ribosome functions, while the pathogenic GMI1000 triggers senescence and phosphorelay  
321 signaling-related stress responses in root hairs<sup>52</sup>. This further supports the special role of root hairs  
322 in differential responses to beneficial and pathogenic microbes in roots. Since both root hairs and  
323 gut microvilli are continually exposed to extremely diverse microbiomes, these cell types might  
324 share similar microbial ecological roles in mediating host-microbiome interactions. Further  
325 molecular and microbial ecological studies in the plant system would advance our understanding of  
326 the rules governing host-microbiome interactions in these "frontline" hair cells.

327

328 Although *Rhizobiaceae* is one of the most well-studied plant symbiotic bacterial families in  
329 leguminous plants, our work suggests that they confer fitness benefits and act as microbiome  
330 network hubs in the non-leguminous plant *Arabidopsis*. A previous study surveyed the core  
331 microbiome compositions across diverse plant lineages, from non-seed to seed plants (31 plant  
332 species), and characterized Bradyrhizobium and Rhizobium as universally plant-enriched core  
333 microbiome taxa<sup>53</sup>. Phylogenetic analysis among 1,314 Rhizobiales genomes suggested that both  
334 nodulating and non-nodulating strains share common genes related to root colonization<sup>54</sup>. The  
335 evolutionarily conserved associations between *Rhizobiaceae* and roots indicate their crucial roles in  
336 the structure and function of root-associated microbiomes. Moreover, a previous study in *Medicago*  
337 suggests that *Rhizobiaceae* are critical hub species in the root microbiome, and that genetic mutants  
338 that loss association with *Rhizobiales* also show altered microbiome structure<sup>55</sup>. Interestingly, in our  
339 non-leguminous *Arabidopsis*, we also detected that enhanced root hair density is associated with  
340 enhanced colonization levels and more edges connected to *Rhizobiaceae* nodes in the microbial co-  
341 abundance network, especially under drought stress. This further suggests the potentially conserved  
342 roles of *Rhizobiaceae* in mediating microbe-microbe interactions in root microbiome network.

343

344 Most mechanistic studies about root-*Rhizobiaceae* interactions were conducted in legume plants<sup>56</sup>.  
345 *Rhizobiaceae* can not only enter root tissues in leguminous roots but also in non-leguminous plants  
346 like rice<sup>57</sup>. This suggests that *Rhizobiaceae* could be endophytes for both leguminous and non-

347 leguminous plants. A recent study systematically surveyed the transcriptome responses to  
348 *Rhizobiaceae* in roots, and found that NAC060 is a key regulator of Rhizobiales specific responses<sup>58</sup>.  
349 More importantly, they identified that host sulfated peptide (phytosulfokine) signaling is essential  
350 for *Rhizobiaceae* mediated growth promoting effects, providing critical insights about the molecular  
351 mechanisms underlying root-Rhizobiales interactions<sup>58</sup>. Considering the powerful genetic and  
352 genomic tools in *Arabidopsis* and *Rhizobiaceae*, this interaction system would likely facilitate new  
353 discoveries about root-commensal interactions.

354

355

### 356 **Material and methods**

#### 357 **Plant material and growth conditions**

358 All the seeds were surface sterilized for 20 minutes with chlorine gas (exposure to 100ml bleach  
359 plus 5ml concentrated hydrochloric) to eliminates potential endophytes<sup>59</sup>. Sterilized seeds were  
360 soaked in a 0.1% agar solution and stored at 4 °C in the dark for 2 days before use. Seeds were  
361 germinated on 1/2x Murashige and Skoog (MS) agar plates with 1% sucrose (12 h light/12 h dark).  
362 7-days-old seedlings were transplanted into pots filled with soil (as described below) in greenhouse.  
363 Plants were grown under a 10 h light (light intensity: 100  $\mu\text{mol m}^{-2} \text{s}^{-1}$ )/14 h dark condition at 22 °C.  
364

#### 365 **Natural soil gorwth substrates**

366 The natural soil used in this study were collected separately from Yuanjiang Savanna Ecosystem  
367 Research Station (E102° 10' ,N23° 28' ) and Xishuangbanna Tropical Botanic Garden (E101°  
368 27' ,N21° 92' ) of Chinese Academy of Sciences. Visible stones, plant debris and litter were  
369 removed before harvesting natural soil. Natural soil was sieved through a 2 mm sieve. Soil from  
370 different locations were thoroughly homogenized and then mixed in a 1:1 ratio as a mixed natural  
371 soil. Finally, we set up a mixture substrate composed of equal volumes (1:1:1:1) of mixed natural  
372 soil, commercial growth roon soil, vermiculite, and perlite as soil substrate for all natural soil  
373 experiments in this study. The soil were scooped into 6cm by 6cm pots in the greenhouse for plants  
374 transplantation. To sterilize natural soil, we autoclaved the substrate twice (at 121 °C for 20 minutes  
375 each time) with at least 24 hours interval between two auto-claving (which thoroughly kills potential  
376 germinated microbe spores after the first time autoclaving). We added fertilizer once per week for  
377 natural soil growth substrates.

378

#### 379 **Drought treatments**

380 Plants were transplanted from plates into natural soil growth substrates at 7 days after germination.  
381 After normal watering for three weeks, plants within each genotype were randomly assigned to  
382 drought and control treatments. We conducted drought treatment by totally withholding watering  
383 and randomly rotating all plants every day.

384

#### 385 **Sample collection**

386 We scooped whole plant outside the pot and removed the soil that was not closely adhered by

shaking the roots<sup>60</sup>. The roots tissue of four plants were immediately cut below the shoot-root junction in a 50 ml Falcon tube filled with 25 ml of sterile PBS (10mM/L). After shaking the Falcon tube for 20 minutes at 180 rpm, the roots were transferred to a new 10 ml Falcon tube filled with fresh PBS. The washing buffer was centrifuged for 20 min at 4000g (16 °C) and the resulting pellet was defined as rhizosphere sample. For root samples collection, roots in fresh PBS were thoroughly washed and sonicated (at 40 Hz for 30s) twice to further discard remaining soil. The pot soil without plant and after removing 2cm of top soil was defined as bulk soil. All the samples were transferred into a new 2 ml tube, immediately frozen in liquid nitrogen, and then stored at -80 °C before DNA extraction.

396

### 397 **DNA extraction and microbiome sequencing**

398 DNA extraction was performed using PowerSoil DNA Isolation Kit (Qiagen, Germany) following  
399 the manufacturer's protocol. The DNA samples that concentration higher than 20 ng/  $\mu$ l were used  
400 for microbiome sequencing. For bacteria amplicon sequencing, the V3-V4 region of the 16s rRNA  
401 gene was amplified with primers 349F 5' -ACTCCTACGGGAGGCAGCA-3' and 806R (5' -  
402 GGAATCTAATGGGTWTCTAAT-3' . Amplification was carried out following thermal conditions:  
403 94°C for 5min, followed by 30 cycles of 94°C for 30 seconds, 52°C for 30 seconds, and 72°C for 30  
404 seconds, with a final extension at 72°C for 10 minutes. Library was prepared following the protocol  
405 of the NEBNext® Ultra™ II DNA Library Prep Kit for Illumina® (New England Biolabs, USA). The  
406 library concentration were determined by Qubit 4.0 Fluorometer. For amplicon sequencing, paired-  
407 end 250 bp sequencing was performed on Illumina Novaseq 6000.

408

### 409 **Microbiome data processing**

410 Raw sequencing reads were filtered using fastp v.0.14.1<sup>61</sup>. The adapter sequences and primers  
411 were further removed using cutadapt v.4.0<sup>62</sup>. Sequencing reads were processed using QIIME2  
412 v.2022.2<sup>63</sup>. Briefly, DADA2 was used to generate a table of unique amplicon sequence variants  
413 (ASV) and their counts per sample<sup>35</sup>. For taxonomic annotation, representative sequences of each  
414 ASV were assigned to the SILVA database (release 138) using pre-trained naive Bayes classifier  
415<sup>64,65</sup>. Unassigned sequences and that annotated as chloroplast and mitochondria (considered as host  
416 contamination) were removed. In addition, the ASV that present in less than 3 samples were also  
417 removed. The retained ASVs were used for downstream analysis.

418

### 419 **Microbial community assembly processes**

420 The null model analysis was carried out to evaluate the microbial community assembly process  
421 by calculating the  $\beta$ -nearest taxon index ( $\beta$ NTI)<sup>38</sup>. Firstly, we calculated the observed abundance-  
422 weighted  $\beta$ -mean-nearest taxon distance ( $\beta$ MNTD<sub>obs</sub>) of pairwise community (sample) with  
423 *comdistnt* function in the "picante" package in R<sup>66</sup>. By randomly shuffling the tips of the  
424 phylogenetic tree, the null model expectation and distribution of  $\beta$ MNTD ( $\beta$ MNTD<sub>null</sub>) were  
425 generated through 999 times randomization. The  $\beta$ NTI were then calculated to quantified the

426 standard deviations that the  $\beta$ MNTD<sub>obs</sub> from the distribution of  $\beta$ MNTD<sub>null</sub> of pairwise community.  
427 When  $|\beta$ NTI| > 2, it is interpreted as the community assembly being governed by deterministic  
428 process. Conversely, when  $|\beta$ NTI| < 2 indicated that community assembly dominated by stochastic  
429 process. Heterogeneous selection and homogeneous selection in deterministic process were  
430 respectively estimated with a value of  $\beta$ NTI > 2 and  $\beta$ NTI < -2<sup>67</sup>.

431 To further assess the contributions of stochastic and deterministic process ( $|\beta$ NTI| < 2) in  
432 community assembly process, a previously developed Raup-Crick index (RC<sub>bray</sub>) were calculated  
433 as described previously<sup>68</sup>. When pairwise community comparison with  $|RC_{bray}| > 0.95$ , indicated  
434 that dispersal lead to a community turnover. When  $RC_{bray} > 0.95$ , the community turnover was  
435 dominated by dispersal limitation, whereas homogenizing dispersal when  $RC_{bray} < -0.95$ . When  
436 pairwise community comparison with  $|\beta$ NTI| < 2 and  $|RC_{bray}| < 0.95$ , community turnover is  
437 estimated to be affected by drift alone. Collectively, the value of  $\beta$ NTI and RC<sub>bray</sub> were integrated  
438 to assess the deterministic and stochastic process in microbial community assembly, as well as  
439 relative influence of the each specific process.

440

#### 441 Metabolome profiling

442 For sample collection, fresh roots of 16 plants grown in the natural soil were harvested as one  
443 biological replicate. Root samples collection steps are same as harvesting root samples for  
444 microbiome sequencing. After sampling, root samples were quickly (within 5 minutes) and  
445 thoroughly washed in 200 ml sterile deionized water. Then root tissue was immediately frozen in  
446 the liquid nitrogen. Tissue fresh weight was recorded and then stored at -80 °C until further  
447 processing.

448 Non-targeted metabolomics were performed to investigate the impact of root hair mutation on  
449 root metabolites under drought condition. Metabolites detection and identification were conducted  
450 using a ultra-performance liquid chromatography (LC-30A, Shimadzu, Japan)-tandem mass  
451 spectrometry (TripleTOF 6600+, SCIEX) system (UPLC-MS/MS) in Wuhan Metware  
452 Biotechnology Co., Ltd. (Wuhan, China) (<http://www.metware.cn/>).

453 For metabolome data processing, principal component analysis (PCA), which implemented by  
454 function prcomp in the “stats” package in R ([www.r-project.org](http://www.r-project.org)), was used to assess differences in  
455 root metabolites among root hair mutants and Col-0. Differential abundance metabolites (DMs)  
456 between each mutant and Col-0 were determined by variable importance in projection (VIP>1), *P*  
457 value (*P* value < 0.05, Student’s t test) and fold change ( $|\log_2 FC| > 0$ ) differences. VIP values were  
458 extracted from Orthogonal Partial Least Squares-Discriminant Analysis (OPLS-DA) result, which  
459 was generated using R package MetaboAnalystR<sup>69</sup>. The heatmap showing the relative abundance  
460 of differential metabolites between mutant and Col-0 were generated by using the  
461 “ComplexHeatmap” package in R<sup>70</sup>. Differential metabolites between mutant and Col-0 were  
462 annotated using KEGG compound database (<http://www.kegg.jp/kegg/compound/>), and further  
463 mapped to KEGG Pathway database (<http://www.kegg.jp/kegg/pathway.html>).

464

465 **Statistics analysis and data visualization**

466 All statistics analyses in present study were conducted in R v.4.1.3 environment (<http://www.r-project.org/>). Before different statistics analysis were chosen, normality tests were performed using  
467 the Shapiro-Wilk test. Then Bartlett's test was used to test for homogeneity of variances using "stats"  
468 package in R. The "vegan" package in R was utilized to assess of alpha and beta diversity of root-  
469 associated microbial community<sup>71</sup>. Specifically, species richness, Shannon diversity were calculated  
470 with *diversity* function. The differences between root hair mutants and Col-0 were assessed using a  
471 one-way ANOVA, followed by an LSD test for multiple comparisons. This analysis was performed  
472 using LSD.test function in "agricolae" package in R<sup>72</sup>. Bray–Curtis distance matrices of microbial  
473 communities were calculated using the *vegdist* function, and principal coordinate analysis (PCoA)  
474 plots were generated accordingly. Permutational multivariate analysis of variance (PERMANOVA)  
475 was performed with the "adonis" function to further assess effects of genotype (Col-0, *gl2* and *rsl2*  
476 *rsl4*), water regime (drought and control), compartment (bulk soil, root and rhizosphere) on  
477 variation of microbiome composition<sup>71</sup>. The "randomForest" and "microeco" packages in R were  
478 utilized to perform differential abundance tests and identify potential marker families among three  
479 genotypes<sup>39,73</sup>. Wilcoxon rank sum test were used to detect the differential (FDR adjust p<0.05)  
480 ASVs (based on relative abundance) between each root hair mutant and Col-0.  
481

482 For network analysis, the ASVs with a relative abundance greater than 0.01% and present in at  
483 least two samples were used for co-occurrence network construction. Spearman correlation  
484 (correlation coefficient >0.7,  $P_{FDR}<0.05$ ) analysis was conducted between paired ASVs using the  
485 "ggClusterNet" packages in R<sup>74</sup>. Network topological parameters, including node and edge counts,  
486 positive and negative correlations, as well as node properties such as degree centrality, closeness  
487 centrality betweenness centrality, were calculated using the "igraph" package in R<sup>75</sup>. Hub nodes  
488 were identified based on all these three measurements of centrality using a log-normal distribution  
489 fit<sup>43</sup>. With the exception of the network visualization, which was conducted in Gephi 0.10<sup>76</sup>, all the  
490 plots in present study were generated using "ggplot2" package in R<sup>77</sup>.

491

492 **Data availability.**

493 All raw 16S amplicon and shotgun metagenomic sequencing data reported in present study will  
494 be deposited in the Sequence Read Archive (<https://www.ncbi.nlm.nih.gov/sra>) upon publication.  
495

496 **Author contributions**

497 Y.S. designed the project, Z.W. and Z.L. conducted experiments with the help from J. Z., X. T.  
498 and K. G. Z.W. analyzed data. Y.S and Z.W. wrote the manuscript.  
499

500 **Acknowledgements**

501 We thank Drs. Hongwei Guo and Yichuan Wang for sharing *gl2* and *rsl2 rsl4* mutants. We are  
502 grateful for Dr. Yajun Chen, Drs. Wenjun Zhou (Xishuangbanna Tropical Botanic Garden(XTBG),  
503 Chinese academy of science), Guojing Wen, and Dixin Yang (Yuanjiang Savanna Ecosystem

504 Research Station, XTBG) for the collection of nature soil. The project was supported by the Stable  
505 Support Plan Program of Shenzhen Natural Science Fund Grant (20220815160107001) and the  
506 NSFC General Project (32270286).

507

508 **Reference.**

- 509 1 Wippel, K. *et al.* Host preference and invasiveness of commensal bacteria in the Lotus and  
510 Arabidopsis root microbiota. *Nat Microbiol* **6**, 1150-1162 (2021). <https://doi.org/10.1038/s41564-021-00941-9>
- 512 2 Steinauer, K. *et al.* Plant diversity effects on soil microbial functions and enzymes are stronger than  
513 warming in a grassland experiment. *Ecology* **96**, 99-112 (2015). <https://doi.org/10.1890/14-0088.1>
- 514 3 Wang, Z. *et al.* Land use intensification in a dry-hot valley reduced the constraints of water content  
515 on soil microbial diversity and multifunctionality but increased CO<sub>2</sub> production. *The Science of  
516 the total environment* **852**, 158397 (2022). <https://doi.org/10.1016/j.scitotenv.2022.158397>
- 517 4 Allsup, C. M., George, I. & Lankau, R. A. Shifting microbial communities can enhance tree  
518 tolerance to changing climates. *Science (New York, N.Y.)* **380**, 835-840 (2023).  
<https://doi.org/10.1126/science.adf2027>
- 520 5 Walters, W. A. *et al.* Large-scale replicated field study of maize rhizosphere identifies heritable  
521 microbes. *Proceedings of the National Academy of Sciences of the United States of America* **115**,  
522 7368-7373 (2018). <https://doi.org/10.1073/pnas.1800918115>
- 523 6 Lundberg, D. S. *et al.* Defining the core Arabidopsis thaliana root microbiome. *Nature* **488**, 86-90  
524 (2012). <https://doi.org/10.1038/nature11237>
- 525 7 Haney, C. H., Samuel, B. S., Bush, J. & Ausubel, F. M. Associations with rhizosphere bacteria can  
526 confer an adaptive advantage to plants. *Nature plants* **1** (2015).  
<https://doi.org/10.1038/nplants.2015.51>
- 528 8 Wang, Z. & Song, Y. Toward understanding the genetic bases underlying plants mediated “cry for  
529 help” to the microbiota. *iMeta* **1**, e8 (2022). <https://doi.org/10.1002/imt2.8>
- 530 9 Zhang, H., Sun, X. & Dai, M. Improving crop drought resistance with plant growth regulators and  
531 rhizobacteria: Mechanisms, applications, and perspectives. *Plant Commun* **3**, 100228 (2022).  
<https://doi.org/10.1016/j.xplc.2021.100228>
- 533 10 Naylor, D., DeGraaf, S., Purdom, E. & Coleman-Derr, D. Drought and host selection influence  
534 bacterial community dynamics in the grass root microbiome. *The ISME journal* **11**, 2691-2704  
535 (2017). <https://doi.org/10.1038/ismej.2017.118>
- 536 11 Santos-Medellin, C., Edwards, J., Liechty, Z., Nguyen, B. & Sundaresan, V. Drought Stress Results  
537 in a Compartment-Specific Restructuring of the Rice Root-Associated Microbiomes. *mBio* **8** (2017).  
<https://doi.org/10.1128/mBio.00764-17>
- 539 12 Santos-Medellín, C. *et al.* Prolonged drought imparts lasting compositional changes to the rice root  
540 microbiome. *Nature Plants* **7**, 1065-1077 (2021). <https://doi.org/10.1038/s41477-021-00967-1>
- 541 13 Xu, L. *et al.* Drought delays development of the sorghum root microbiome and enriches for  
542 monoderm bacteria. *Proceedings of the National Academy of Sciences of the United States of  
543 America* **115**, E4284-e4293 (2018). <https://doi.org/10.1073/pnas.1717308115>
- 544 14 Xu, L. *et al.* Genome-resolved metagenomics reveals role of iron metabolism in drought-induced  
545 rhizosphere microbiome dynamics. *Nature communications* **12**, 3209 (2021).  
<https://doi.org/10.1038/s41467-021-23553-7>
- 547 15 Fitzpatrick, C. R. *et al.* Assembly and ecological function of the root microbiome across angiosperm

548 plant species. *Proceedings of the National Academy of the Sciences of the United States of America*  
549 **115**, E1157-E1165 (2018). <https://doi.org/10.1073/pnas.1717617115>

550 16 Xu, L. *et al.* Drought delays development of the sorghum root microbiome and enriches for  
551 monoderm bacteria. *Proceedings of the National Academy of the Sciences of the United States of*  
552 *America* **115**, E4284-E4293 (2018). <https://doi.org/10.1073/pnas.1717308115>

553 17 Naumann, G. *et al.* Global Changes in Drought Conditions Under Different Levels of Warming.  
554 *Geophysical Research Letters* **45**, 3285-3296 (2018). <https://doi.org/10.1002/2017gl076521>

555 18 de Vries, F. T., Griffiths, R. I., Knight, C. G., Nicolitch, O. & Williams, A. Harnessing rhizosphere  
556 microbiomes for drought-resilient crop production. *Science (New York, N.Y.)* **368**, 270-274 (2020).  
557 <https://doi.org/10.1126/science.aaz5192>

558 19 Song, Y. *et al.* FERONIA restricts Pseudomonas in the rhizosphere microbiome via regulation of  
559 reactive oxygen species. *Nature plants* **7**, 644-654 (2021). <https://doi.org/10.1038/s41477-021-00914-0>

560 20 Lebeis, S. L. *et al.* Salicylic acid modulates colonization of the root microbiome by specific bacterial  
561 taxa. *Science (New York, N.Y.)* **349**, 860-864 (2015). <https://doi.org/10.1126/science.aaa8764>

562 21 Chen, T. *et al.* A plant genetic network for preventing dysbiosis in the phyllosphere. *Nature* (2020).  
563 <https://doi.org/10.1038/s41586-020-2185-0>

564 22 Pfeilmeier, S. *et al.* The plant NADPH oxidase RBOHD is required for microbiota homeostasis in  
565 leaves. *Nature Microbiology* **6**, 852-864 (2021). <https://doi.org/10.1038/s41564-021-00929-5>

566 23 Vilchez, J. I. *et al.* DNA demethylases are required for myo-inositol-mediated mutualism between  
567 plants and beneficial rhizobacteria. *Nature plants* **6**, 983-995 (2020).  
568 <https://doi.org/10.1038/s41477-020-0707-2>

569 24 Lv, S. *et al.* Dysfunction of histone demethylase IBM1 in Arabidopsis causes autoimmunity and  
570 reshapes the root microbiome. *The ISME journal* **16**, 2513-2524 (2022).  
571 <https://doi.org/10.1038/s41396-022-01297-6>

572 25 Kaushal, R. *et al.* Dicer-like proteins influence Arabidopsis root microbiota independent of RNA-  
573 directed DNA methylation. *Microbiome* **9**, 57 (2021). <https://doi.org/10.1186/s40168-020-00966-y>

574 26 Huang, A. C. *et al.* A specialized metabolic network selectively modulates Arabidopsis root  
575 microbiota. *Science (New York, N.Y.)* **364** (2019). <https://doi.org/10.1126/science.aau6389>

576 27 Stringlis, I. A. *et al.* MYB72-dependent coumarin exudation shapes root microbiome assembly to  
577 promote plant health. *Proceedings of the National Academy of Sciences of the United States of*  
578 *America* **115**, E5213-E5222 (2018). <https://doi.org/10.1073/pnas.1722335115>

579 28 Ruiz, S. *et al.* Significance of root hairs at the field scale - modelling root water and phosphorus  
580 uptake under different field conditions. *Plant Soil* **447**, 281-304 (2020).  
581 <https://doi.org/10.1007/s11104-019-04308-2>

582 29 Zhang, X. *et al.* The spatial distribution of rhizosphere microbial activities under drought: water  
583 availability is more important than root-hair controlled exudation. *New Phytologist* (2022).  
584 <https://doi.org/10.1111/nph.18409>

585 30 Holz, M., Zarebanadkouki, M., Kuzyakov, Y., Pausch, J. & Carminati, A. Root hairs increase  
586 rhizosphere extension and carbon input to soil. *Annals of Botany* **121**, 61-69 (2018).  
587 <https://doi.org/10.1093/aob/mcx127>

588 31 Lin, Q. *et al.* GLABRA2 Directly Suppresses Basic Helix-Loop-Helix Transcription Factor Genes  
589 with Diverse Functions in Root Hair Development. *Plant Cell* **27**, 2894-2906 (2015).  
590 <https://doi.org/10.1105/tpc.15.00607>

591

592 32 Pires, N. D. *et al.* Recruitment and remodeling of an ancient gene regulatory network during land  
593 plant evolution. *Proceedings of the National Academy of Sciences of the United States of America*  
594 **110**, 9571-9576 (2013). <https://doi.org/10.1073/pnas.1305457110>

595 33 Yi, K., Menand, B., Bell, E. & Dolan, L. A basic helix-loop-helix transcription factor controls cell  
596 growth and size in root hairs. *Nat Genet* **42**, 264-267 (2010). <https://doi.org/10.1038/ng.529>

597 34 Alonso, J. M. *et al.* Genome-wide insertional mutagenesis of *Arabidopsis thaliana*. *Science* **301**,  
598 653-657 (2003). <https://doi.org/10.1126/science.1086391>

599 35 Callahan, B. J. *et al.* DADA2: High-resolution sample inference from Illumina amplicon data. *Nat  
600 Methods* **13**, 581-583 (2016). <https://doi.org/10.1038/nmeth.3869>

601 36 Xu, L. *et al.* Drought delays development of the sorghum root microbiome and enriches for  
602 monoderm bacteria. *Proceedings of the National Academy of the Sciences of the United States of  
603 America* **115**, E4284-E4293 (2018). <https://doi.org/10.1073/pnas.1717308115>

604 37 Gao, C. *et al.* Co-occurrence networks reveal more complexity than community composition in  
605 resistance and resilience of microbial communities. *Nature communications* **13** (2022).  
606 <https://doi.org/10.1038/s41467-022-31343-y>

607 38 Stegen, J. C., Lin, X., Konopka, A. E. & Fredrickson, J. K. Stochastic and deterministic assembly  
608 processes in subsurface microbial communities. *ISME J* **6**, 1653-1664 (2012).  
609 <https://doi.org/10.1038/ismej.2012.22>

610 39 Liu, C., Cui, Y., Li, X. & Yao, M. microeco: an R package for data mining in microbial community  
611 ecology. *FEMS Microbiology Ecology* **97** (2020). <https://doi.org/10.1093/femsec/fiaa255>

612 40 Faust, K. & Raes, J. Microbial interactions: from networks to models. *Nat Rev Microbiol* **10**, 538-  
613 550 (2012). <https://doi.org/10.1038/nrmicro2832>

614 41 Banerjee, S., Schlaeppi, K. & van der Heijden, M. G. A. Keystone taxa as drivers of microbiome  
615 structure and functioning. *Nat Rev Microbiol* **16**, 567-576 (2018). [https://doi.org/10.1038/s41579-018-0024-1](https://doi.org/10.1038/s41579-<br/>616 018-0024-1)

617 42 Barberan, A., Bates, S. T., Casamayor, E. O. & Fierer, N. Using network analysis to explore co-  
618 occurrence patterns in soil microbial communities. *ISME J* **6**, 343-351 (2012).  
619 <https://doi.org/10.1038/ismej.2011.119>

620 43 Agler, M. T. *et al.* Microbial Hub Taxa Link Host and Abiotic Factors to Plant Microbiome Variation.  
621 *PLOS Biology* **14**, e1002352 (2016). <https://doi.org/10.1371/journal.pbio.1002352>

622 44 Schafer, M. *et al.* Metabolic interaction models recapitulate leaf microbiota ecology. *Science* **381**,  
623 eadf5121 (2023). <https://doi.org/10.1126/science.adf5121>

624 45 O'Banion, B. S. *et al.* Plant myo-inositol transport influences bacterial colonization phenotypes.  
625 *Current Biology* (2023). <https://doi.org/10.1016/j.cub.2023.06.057>

626 46 He, D. *et al.* Flavonoid-attracted *Aeromonas* sp. from the *Arabidopsis* root microbiome enhances  
627 plant dehydration resistance. *ISME J* (2022). <https://doi.org/10.1038/s41396-022-01288-7>

628 47 Hassan, S. & Mathesius, U. The role of flavonoids in root-rhizosphere signalling: opportunities and  
629 challenges for improving plant-microbe interactions. *Journal of Experimental Botany* **63**, 3429-  
630 3444 (2012). <https://doi.org/10.1093/jxb/err430>

631 48 Bakker, P., Pieterse, C. M. J., de Jonge, R. & Berendsen, R. L. The Soil-Borne Legacy. *Cell* **172**,  
632 1178-1180 (2018). <https://doi.org/10.1016/j.cell.2018.02.024>

633 49 Brown, L. K., George, T. S., Dupuy, L. X. & White, P. J. A conceptual model of root hair ideotypes  
634 for future agricultural environments: what combination of traits should be targeted to cope with  
635 limited P availability? *Annals of Botany* **112**, 317-330 (2012). <https://doi.org/10.1093/aob/mcs231>

636 50 Saengwilai, P. *et al.* Root hair phenotypes influence nitrogen acquisition in maize. *Annals of Botany*  
637 **128**, 849-858 (2021). <https://doi.org/10.1093/aob/mcab104>

638 51 Verbon, E. H. *et al.* Cell-type-specific transcriptomics reveals that root hairs and endodermal  
639 barriers play important roles in beneficial plant-rhizobacterium interactions. *Mol Plant* **16**, 1160-  
640 1177 (2023). <https://doi.org/10.1016/j.molp.2023.06.001>

641 52 Yang, Q. *et al.* Comparative single-nucleus RNA-seq analysis captures shared and distinct responses  
642 to beneficial and pathogenic microbes in roots. *bioRxiv*, 2023.2008. 2003.551619 (2023).

643 53 Yeoh, Y. K. *et al.* Evolutionary conservation of a core root microbiome across plant phyla along a  
644 tropical soil chronosequence. *Nature communications* **8**, 215 (2017).  
<https://doi.org/10.1038/s41467-017-00262-8>

645 54 Garrido-Oter, R. *et al.* Modular Traits of the Rhizobiales Root Microbiota and Their Evolutionary  
646 Relationship with Symbiotic Rhizobia. *Cell host & microbe* **24**, 155-167 e155 (2018).  
<https://doi.org/10.1016/j.chom.2018.06.006>

647 55 Wang, X. *et al.* Mycorrhizal symbiosis modulates the rhizosphere microbiota to promote rhizobia-  
648 legume symbiosis. *Mol Plant* **14**, 503-516 (2021). <https://doi.org/10.1016/j.molp.2020.12.002>

649 56 Yang, J. *et al.* Mechanisms underlying legume-rhizobium symbioses. *Journal of integrative plant  
650 biology* **64**, 244-267 (2022). <https://doi.org/10.1111/jipb.13207>

651 57 Perrine-Walker, F. M., Prayitno, J., Rolfe, B. G., Weinman, J. J. & Hocart, C. H. Infection process  
652 and the interaction of rice roots with rhizobia. *J Exp Bot* **58**, 3343-3350 (2007).  
<https://doi.org/10.1093/jxb/erm181>

653 58 Hucklenbroich, J. *et al.* Rhizobiales commensal bacteria promote *Arabidopsis thaliana* root growth  
654 via host sulfated peptide pathway. *bioRxiv*, 2021.2005. 2025.444716 (2021).

655 59 Haney, C. H., Samuel, B. S., Bush, J. & Ausubel, F. M. Associations with rhizosphere bacteria can  
656 confer an adaptive advantage to plants. *Nature Plants* **1**, 1-9 (2015).  
<https://doi.org/10.1038/nplants.2015.51>

657 60 Bulgarelli, D. *et al.* Revealing structure and assembly cues for *Arabidopsis* root-inhabiting bacterial  
658 microbiota. *Nature* **488**, 91-95 (2012). <https://doi.org/10.1038/nature11336>

659 61 Chen, S., Zhou, Y., Chen, Y. & Gu, J. fastp: an ultra-fast all-in-one FASTQ preprocessor.  
660 *Bioinformatics* **34**, i884-i890 (2018).

661 62 Martin, M. Cutadapt removes adapter sequences from high-throughput sequencing reads. *2011* **17**,  
662 3 (2011). <https://doi.org/10.14806/ej.17.1.200>

663 63 Bolyen, E. *et al.* Reproducible, interactive, scalable and extensible microbiome data science using  
664 QIIME 2. *Nature Biotechnology* **37**, 852-857 (2019). <https://doi.org/10.1038/s41587-019-0209-9>

665 64 Quast, C. *et al.* The SILVA ribosomal RNA gene database project: improved data processing and  
666 web-based tools. *Nucleic Acids Res* **41**, D590-596 (2013). <https://doi.org/10.1093/nar/gks1219>

667 65 Wang, Q., Garrity, G. M., Tiedje, J. M. & Cole, J. R. Naive Bayesian classifier for rapid assignment  
668 of rRNA sequences into the new bacterial taxonomy. *Appl Environ Microbiol* **73**, 5261-5267 (2007).  
<https://doi.org/10.1128/aem.00062-07>

669 66 Kembel, S. W. *et al.* Picante: R tools for integrating phylogenies and ecology. *Bioinformatics* **26**,  
670 1463-1464 (2010). <https://doi.org/10.1093/bioinformatics/btq166>

671 67 Jizhong, Z. & Daliang, N. Stochastic Community Assembly: Does It Matter in Microbial Ecology?  
672 *Microbiology and Molecular Biology Reviews* (2017). <https://doi.org/10.1128/MMBR>

673 68 Stegen, J. C. *et al.* Quantifying community assembly processes and identifying features that impose  
674 them. *ISME J* **7**, 2069-2079 (2013). <https://doi.org/10.1038/ismej.2013.93>

680 69 Chong, J. & Xia, J. MetaboAnalystR: an R package for flexible and reproducible analysis of  
 681 metabolomics data. *Bioinformatics* **34**, 4313-4314 (2018).  
<https://doi.org/10.1093/bioinformatics/bty528>

682 70 Gu, Z. Complex heatmap visualization. *iMeta* **1** (2022). <https://doi.org/10.1002/imt2.43>

683 71 Jari Oksanen *et al.* vegan: Community Ecology Package, R package version (2013).

684 72 de Mendiburu, F. & de Mendiburu, M. F. Package ‘agricolae’. *R Package, version 1* (2019).

685 73 Liaw, A. & Wiener, M. Classification and regression by randomForest. *R News* **2**, 18-22 (2002).

686 74 Wen, T. *et al.* ggClusterNet: An R package for microbiome network analysis and modularity-based  
 687 multiple network layouts. *iMeta* **1** (2022). <https://doi.org/10.1002/imt2.32>

688 75 Csárdi, G. & Nepusz, T. The igraph software package for complex network research. *InterJournal, Complex Systems* **1965**, 1-9 (2006).

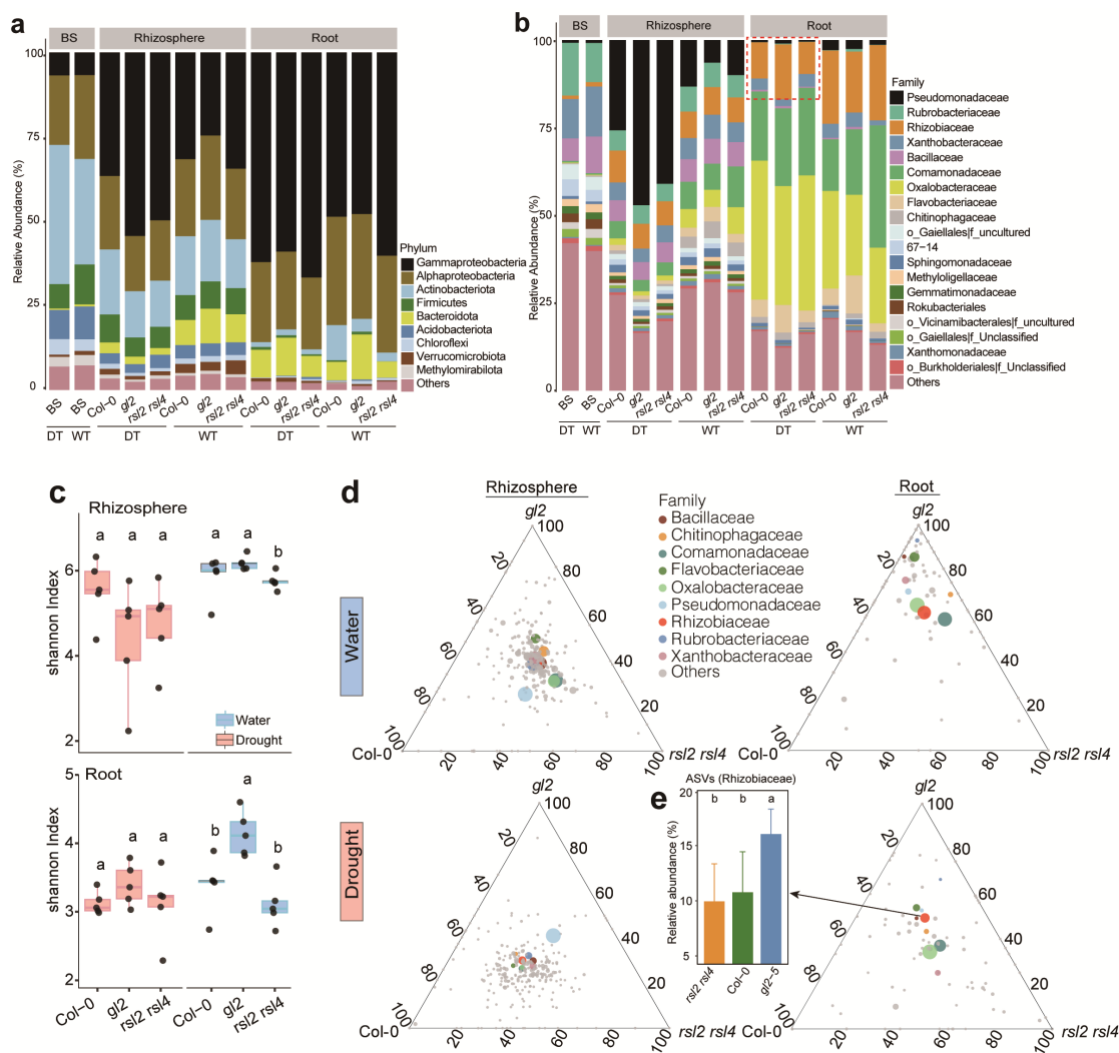
689 76 Bastian, M., Heymann, S. & Jacomy, M. Gephi: an open source software for exploring and  
 690 manipulating networks. *Proceedings of the international AAAI conference on web and social media*  
 691 **3**, 361-362 (2009). [https://doi.org/https://doi.org/10.1609/icwsm.v3i1.13937](https://doi.org/10.1609/icwsm.v3i1.13937)

692 77 Wickham, H. ggplot2: Elegant Graphics for Data Analysis. *Springer-Verlag New York* (2016).

693

694

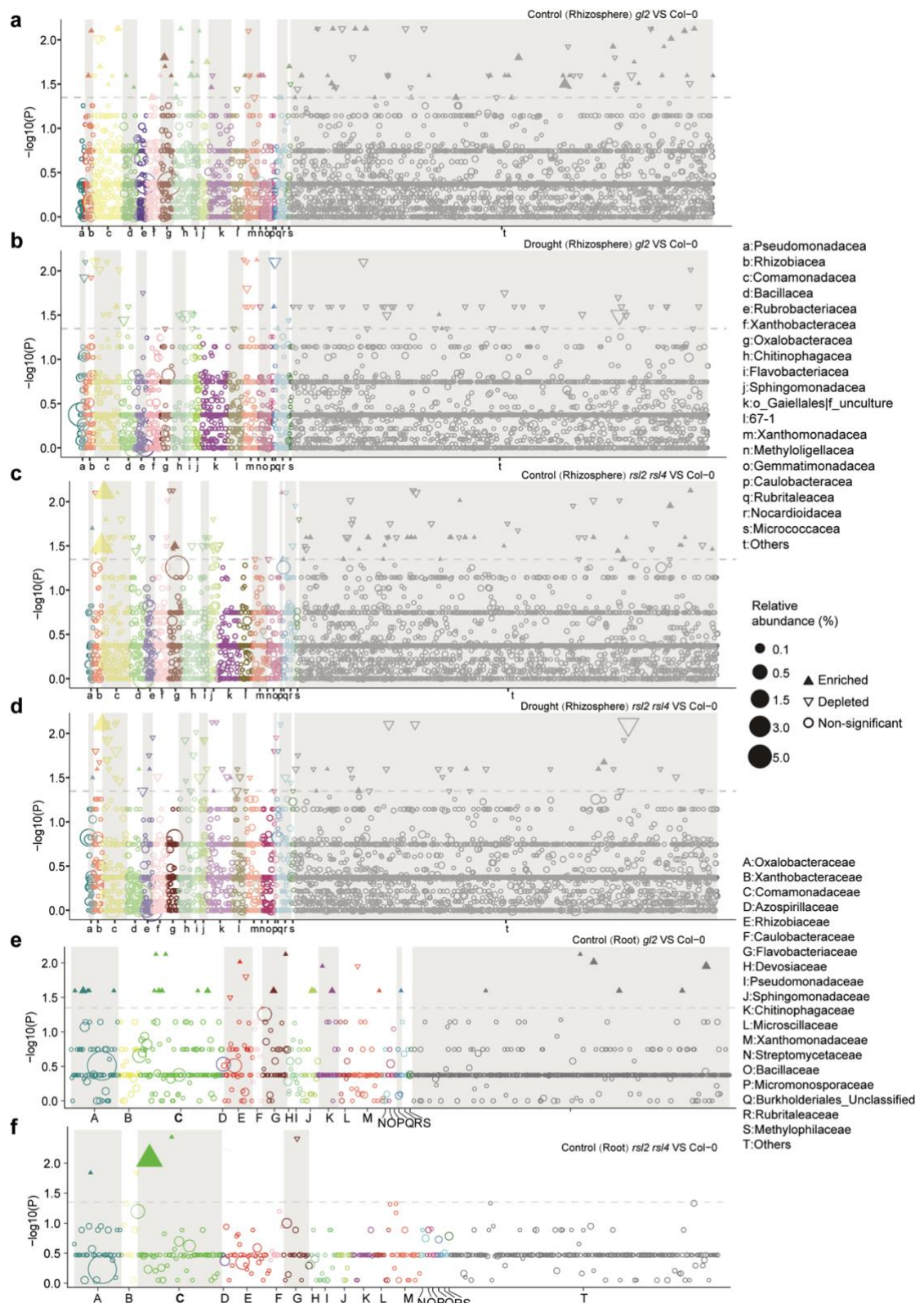
695  
 696 **Supplementary Figure**



697  
 698 **Supplementary Fig. 1.** a-b Relative abundance of phyla (a) and family (b) level compositions in the root,  
 699

699 rhizosphere and bulk soil microbiomes under control and drought conditions. c Shannon index of microbial  
700 communities in both root and rhizosphere samples. Lowercase letters indicate the significant ( $P < 0.05$  corrected  
701 using Bonferroni method, one-way ANOVA followed by LSD test) differences among genotypes. d Ternary plot of  
702 relative abundance-based families detected in the roots of Col-0, *gl2*, and *rsl2 rsl4*. Each circle represents each family.  
703 Different colors represent different families. e Accumulation of relative abundance of ASVs belonging to  
704 *Rhizobiaceae* increased with root hair density. Data are represented as mean (bar)  $\pm$  standard error of mean (error  
705 bar). Different letters represent the significant ( $p < 0.05$  corrected using Bonferroni method, one-way ANOVA  
706 followed by LSD test) differences among genotypes.

707

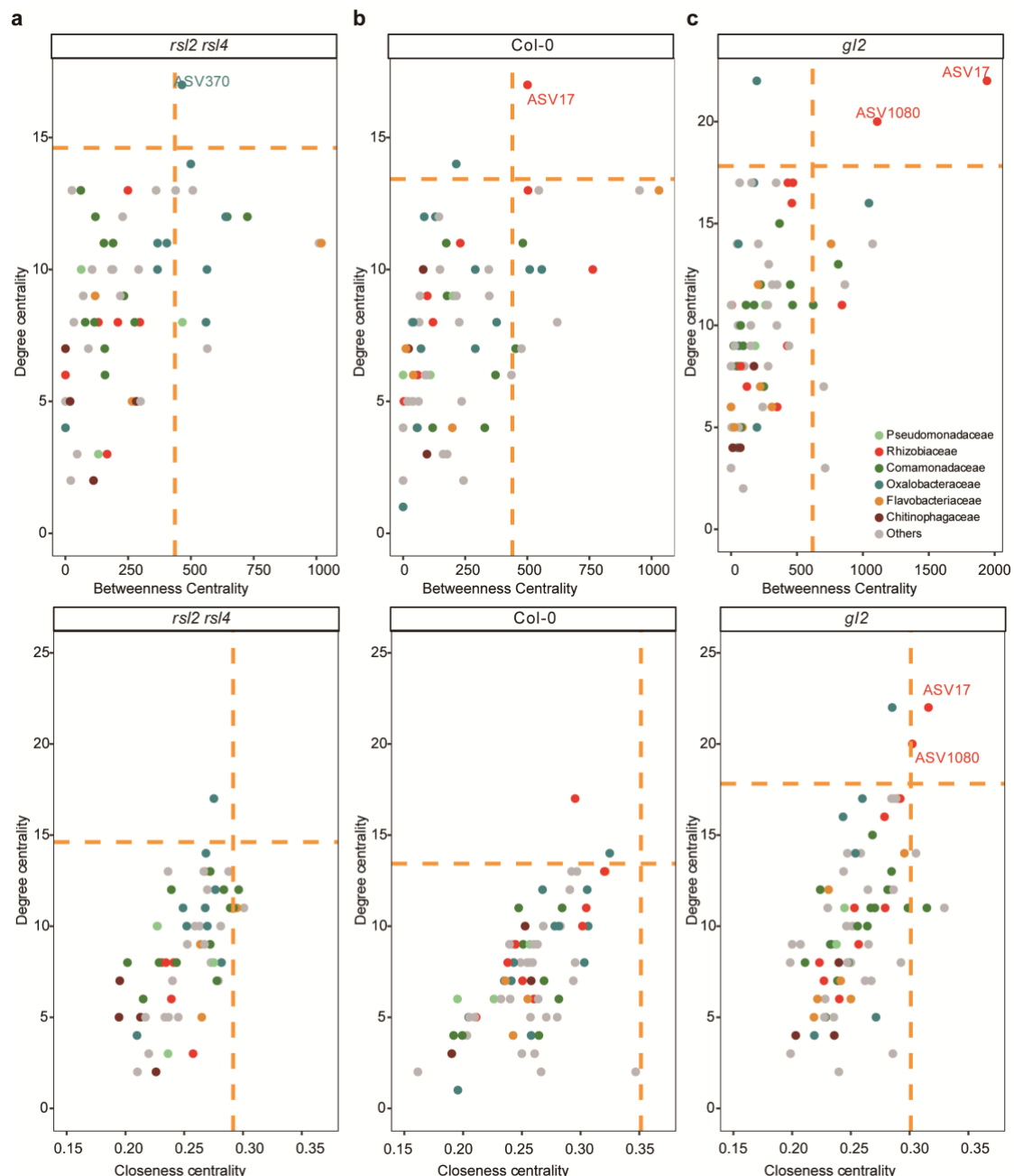


708

709 **Supplementary Fig. 2.** Manhattan plot showing the differentially abundant ASVs (DA-ASVs) enriched (Wilcoxon  
 710 rank sum test, the dotted line indicates unadjusted  $P < 0.05$ ) in the rhizosphere samples (**a-d**) or roots (**f-g**) of *rs1/2*  
 711 or *gl2* or *Col-0* under control and drought conditions (n=5 replicates for each individual group). Each dot and  
 712 ASVs were colored according to the taxonomic families. Size of each dot or triangle  
 713 represent the relative abundance of each ASV. Solid upward triangles indicate that ASV enriched in the roots of

714 mutant. Hollow downward triangles represent that ASV depleted in the mutants.

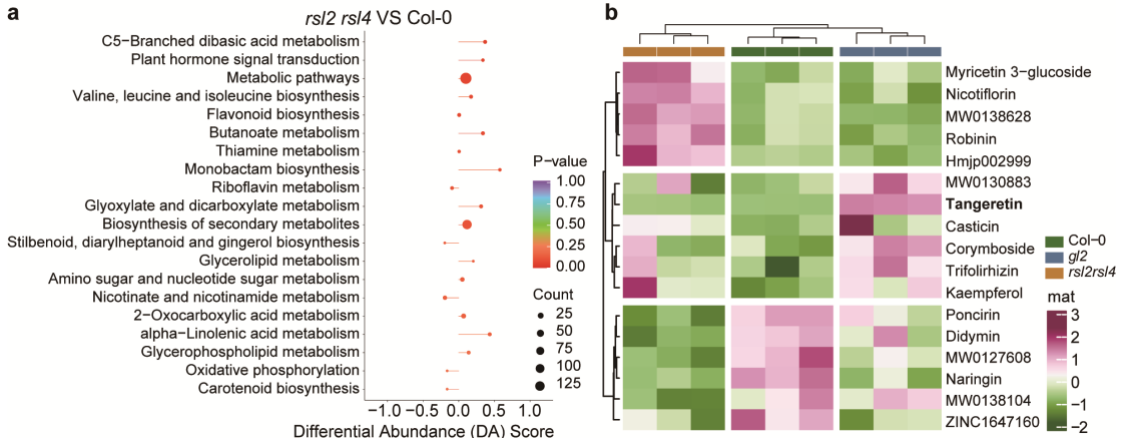
715



716

717 **Supplementary Fig. 3** Microbial hub nodes (ASVs) within the root microbial community were identified in each  
718 co-occurrence networks under drought stress (related to Fig. 2d-f). Hub nodes were identified based on all three  
719 measurements of centrality (include degree, closeness centrality, and betweenness centrality). Different colors  
720 represent nodes belonging to different family. The hub ASVs were labeled. Yellow line:  $p = 0.1$  based on a log-  
721 normal distribution fit.

722



723

724 **Supplementary Fig. 4** Metabolome profiling of mutants affecting root hair densities. **a** Enriched pathways of DMs  
 725 between the roots of *rsl2 rsl4* mutant and Col-0 under drought condition. The differential abundance (DA) score  
 726 represents the changes in DMs within each pathway in the roots of *rsl2 rsl4* compared to Col-0. A score of -1 and 1  
 727 represent that all the DMs in the pathway were downregulated and upregulated, respectively. **b** Heat map showed  
 728 the differences of relative content (log) of all differential flavonoids between the root hair mutant and Col-0.

729